



## Letter

## Synthesis of ZnO clusters within ZSM-5 crystals by thermal diffusion method

Jian Wu, Yunshuai Shang, Yang Yang, Yu Wang, Jiang Zhu, Changgong Meng\*

Department of Chemistry, Dalian University of Technology, Dalian 116024, China

## ARTICLE INFO

## Article history:

Received 22 September 2009

Received in revised form 8 April 2010

Accepted 14 April 2010

Available online 22 April 2010

## Keywords:

Inorganic materials

Optical materials

Semiconductors

Luminescence

X-ray diffraction

## ABSTRACT

The thermal diffusion method is employed for ZnO loading into ZSM-5 crystals (ca. 120  $\mu\text{m}$  along  $c$  axis) which is regarded as a good host material for guest encapsulation. Optical microscopy photographs and X-ray powder diffraction spectra are obtained and show that the ZnO clusters are infiltrated into ZSM-5 crystals, instead of locating on the surface of the crystals. An intense porosity analysis based on density functional theory is used to illustrate the pore texture of the ZnO-loaded samples. The sample prepared at 650 °C has ZnO clusters existing mainly in the external surface of ZSM-5. As for the sample prepared at 750 °C, the micropores of ZSM-5 have been occupied.

© 2010 Elsevier B.V. All rights reserved.

## 1. Introduction

Zinc oxide attracts much attention for its wide band-gap (3.37 eV, 298 K) and large exciton binding energy (ca. 60 meV). In recent years, many works have been focused on preparing and characterizing of zinc oxide nano- or subnano-particles which process wide potential applications, such as transparent electrodes, gas sensors, acousto-optical devices and piezoelectric devices [1–5]. However, nano- or subnano-particles are unstable due to their high surface energy [6,7] and could be agglomerated into large ones which are deprived of the small particles' properties. Many materials, such as colloidal, porous glasses, certain polymers and molecular sieves are used as hard templates to make the mall particles stabilized [8].

Molecular sieves, whose structures define regular channels and cages, have been considered to be a promising host material for accommodating some semiconductor guests [9–11]. Specifically, researchers have been dedicated to infiltrate ZnO species into the pores of molecular sieves in the past few years and made a good progress in both structures and optical properties. Wang et al. [8] put ZnO clusters into the micropores of zeolite L by incipient wetness impregnation method and found a blue shift on the photoluminescence (PL) spectra, which could be ascribed to the quantum size effect. Lim and Ryu [12] made ZnO nanoclusters incorporated into TMA-A zeolite and observed ZnO nanoclusters by HR-TEM. Bouvy et al. [13] used CMI-1 mesoporous material as the host to

accommodate ZnO into the pores. In their study, quantum size effect was also demonstrated, furthermore, an efficient random laser was observed originating from the amplification of stimulated emission of ZnO implying a two-photon absorption process.

The selectivity of host material is vital to the optical properties of the so-prepared host-guest material, accounting for the substantial light scattering of powder-like material. In our study, ZSM-5 crystals are employed, as the host, for impregnating ZnO within it. A thermal diffusion method has been applied during the process. Intensive porosity analysis to the original ZSM-5 and ZnO-loaded samples have been carried out with nitrogen adsorption data at  $-196^\circ\text{C}$ , by which the pore textures of all samples are well described. It is shown that the crystal-based material is appropriate to the optical applications due to its good photoluminescence and high optical transmittance.

## 2. Material and methods

The host ZSM-5 crystals were hydrothermally synthesized and post-treated as our previous work reported [14]. ZnO was impregnated into ZSM-5 crystals by two steps. Firstly, the molecular sieve crystals (0.3 g) were dehydrated at  $110^\circ\text{C}$  for 1 h and put into a small glass tube (G1,  $\Phi = 6.84\text{ mm}$ ) with one side open. A Pyrex glass tube (G2,  $\Phi = 12.10\text{ mm}$ ) was filled with 2 g Zn powder. Then the G1 tube was set into G2 and sealed to form the main thermal diffusion reactor. After that, the reactor was heated at 650 or  $750^\circ\text{C}$  for 20 h, with a heating rate of less than  $1^\circ\text{C}/\text{min}$ . When the reactor was cooled down to the ambient temperature, the crystals were taken out, transferred into a crucible and calcined in air at  $550^\circ\text{C}$  to get all the zinc species into oxides. The samples prepared at 650 and  $750^\circ\text{C}$  are labeled as Z650 and Z750, respectively.

ZnO/ZSM-5 was characterized by a Shimadzu XRD-6000 diffractometer, using  $\text{CuK}\alpha$  ( $\lambda = 1.5406\text{ \AA}$ ) radiation source (40 kV, 30 mA) with the scanning rate of  $0.03^\circ/\text{s}$ . The photographs of samples were pictured on Leica DMLP polarization microscope. The ZnO contents of all samples were detected by Varian Vista-Pro ICP-OES spectrometer. The surface area and porosity properties were calculated by nitrogen

\* Corresponding author. Tel.: +86 411 84708545; fax: +86 411 84708545.

E-mail addresses: [wujiandut@163.com](mailto:wujiandut@163.com) (J. Wu), [cgmeng@dlut.edu.cn](mailto:cgmeng@dlut.edu.cn) (C. Meng).

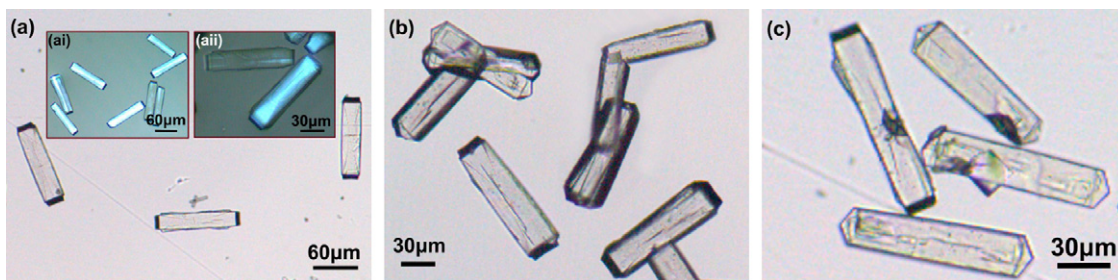


Fig. 1. Optical microscope images of samples: (a) ZSM-5, (b) Z650, (c) Z750; (ai) and (a(ii)) polarizing microscopy image of ZSM-5 crystals.

adsorption data at  $-196^{\circ}\text{C}$  using a Micromeritics ASAP-2020 porosity analyzer. The density functional theory (DFT) model was employed to evaluate the pore distribution, cumulative pore volume and total area in pores. The PL spectra were recorded at room temperature on PerkinElmer LS-55 instrument, using a xenon lamp as the excitation source.

### 3. Results and discussion

#### 3.1. Morphology and chemical composition

The granule size of ZSM-5 crystal reaches about  $120\text{ }\mu\text{m}$  along  $c$  axis (Fig. 1), which has good optical transmittance property. As shown in Fig. 1(a(ii)), through a beam of polarized light, the image well describes the “hourglass” pattern of the crystal. ZSM-5 and ZnO-loaded crystals are transparent, besides, none of ZnO macro-crystalline particles are observed on the crystal surface, which is

thereby a promising material for optical studies and applications. However, the crystals after treatment at  $750^{\circ}\text{C}$  tend to be rifted in a certain degree, which thereby decrease the quality of the crystal and means that the treatment condition for sample Z750 is tough for thermal diffusion process.

The chemical compositions of the samples are listed in Table 1. The ZnO content in Z750 sample is more than that in Z650, resulting from the different heating temperature during the preparing process which thereby affects the vapor pressure of Zn (gas) in the reactor.

#### 3.2. Crystal phase analysis

X-ray powder diffraction (XRD) analysis has been done to evaluate the variety of crystal phase during the thermal diffusion process.

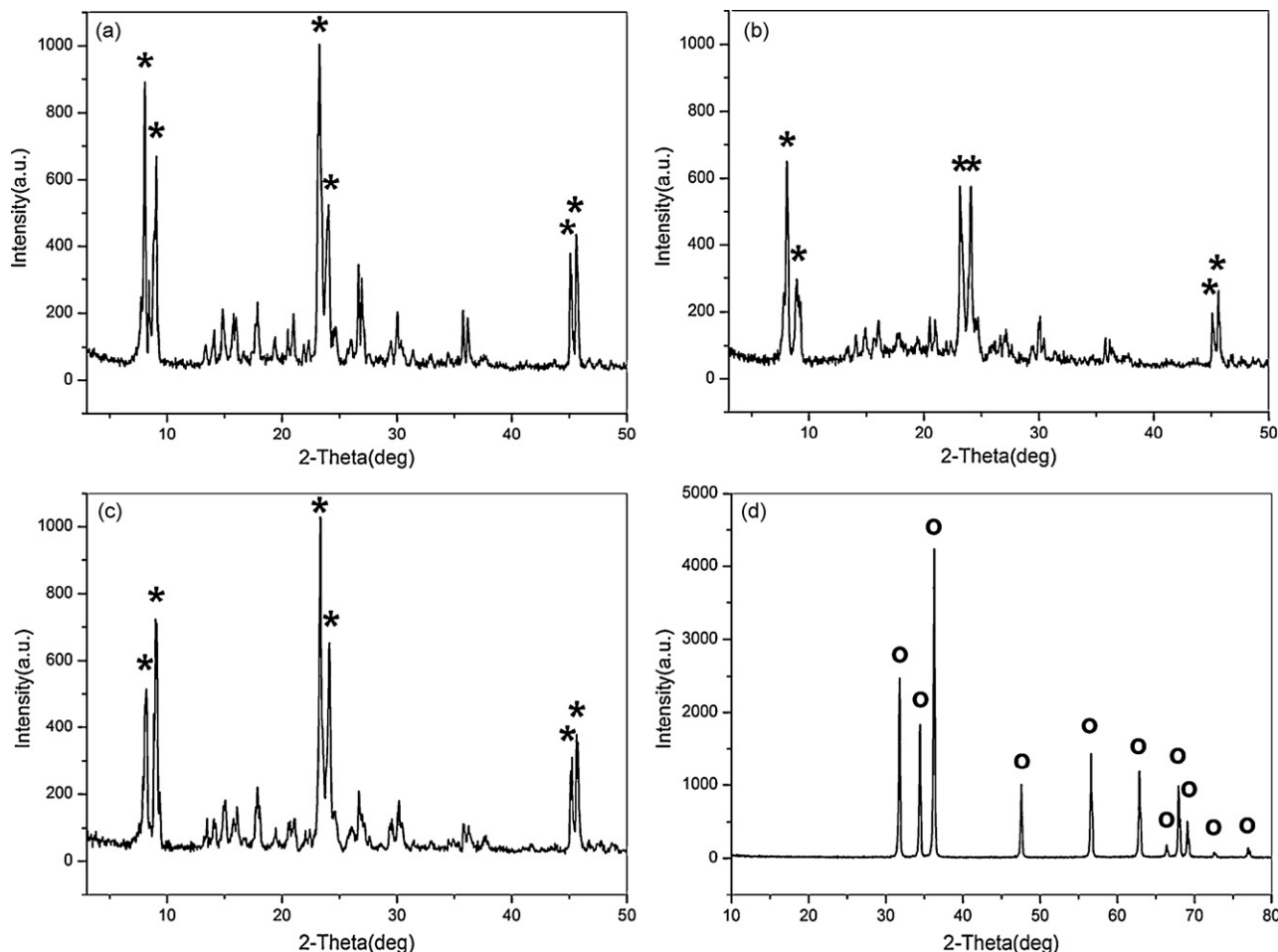


Fig. 2. XRD patterns of samples and ZnO reagent: (a) Z650, (b) Z750, (c) ZSM-5, (d) ZnO reagent; characteristic peak indexed: (\*) ZSM-5, (○) ZnO.

**Table 1**  
Chemical content and micropore properties of samples.

Sample ID	ZnO content in sample (wt.%)	$V_{\text{micro}}^a$ ( $\text{cm}^3 \text{g}^{-1}$ )	$S_{\text{micro}}^b$ ( $\text{m}^2 \text{g}^{-1}$ )
ZSM-5	–	0.124	485
Z650	0.93	0.123	480
Z750	2.22	0.108	95

<sup>a</sup> Total volume in micropores for pore diameter less than 1.358 nm (DFT).

<sup>b</sup> Surface area in micropores for pore diameter larger than 0.465 nm (DFT).

As shown in Fig. 2(a–c), the MFI structure (IUPAC nomenclature) remains essentially unchanged after ZnO introducing. However, a manifest decrement in the characteristic diffraction peaks appears, especially in sample Z750, since the high reaction temperature affects the integrity of some crystal faces. Furthermore, compared against the XRD pattern of zinc oxide reagent, no evident reflection peaks of ZnO are found in XRD patterns of ZnO-loaded samples, which attributes to the trace amount of ZnO in the samples and none of ZnO bulk aggregates locating outside ZSM-5 crystals.

### 3.3. Physisorption analysis

The adsorption isotherms of these samples (Fig. 3(a–c)) exhibit type I as Brunauer–Deming–Deming–Teller (BDDT) classification [15], indicating the characteristic of a microporous material. A hysteresis loop appears (Fig. 3(a–c)) when the relative pressure ( $P/P^0$ ),  $P$  refers the dosing pressure of nitrogen when measuring,  $P^0$  is

the standard atmospheric pressure) reaches beyond 0.1, which is caused by a transition of fluid-like to a solid-like adsorbate phase when the secondary adsorption in the wider channel intersections, i.e., the external surface of ZSM-5 [16].

The low pressure adsorption data are well fitted with DFT model as displayed in Fig. 3(ai, bi, ci), which describes the micropore properties of samples. The DFT fitted isotherm of Z650 is almost the same as the original ZSM-5 crystal, illustrating that the ZnO clusters do not intrude into the micropores of ZSM-5 here but stand in the external surface. When the ZnO content is increasing (Z750), the adsorption capacity turns lower (about 11.7%) than that of ZSM-5 crystals, demonstrating that ZnO clusters have occupied the micropores of ZSM-5 or blocked the pore window under this condition.

DFT method has been applied to analyze the pore size distribution by calculated from the low pressure nitrogen adsorption data. Fig. 3d depicts the pore size distribution of ZSM-5 and ZnO-loaded ZSM-5. The main pore size of ZSM-5 sample appears at about 0.58 nm. When the ZnO content is low (Z650), the main pore size is the same as the original ZSM-5, at about 0.58 nm. It is shown that the guest clusters are not locating in the micropores. Moreover, when the ZnO content is high (Z750), the main pore size distribution peak disappears, which indicates that the micropores have been blocked. At the same time, a new peak at 0.68 nm, as well as a shoulder band larger than 0.68 nm, has been found. It may be due to the producing of new micropores, generated from partially filled channels of ZSM-5 by ZnO clusters. Another possible mechanism for new micropores' formation is the arrangement of ZnO cluster,

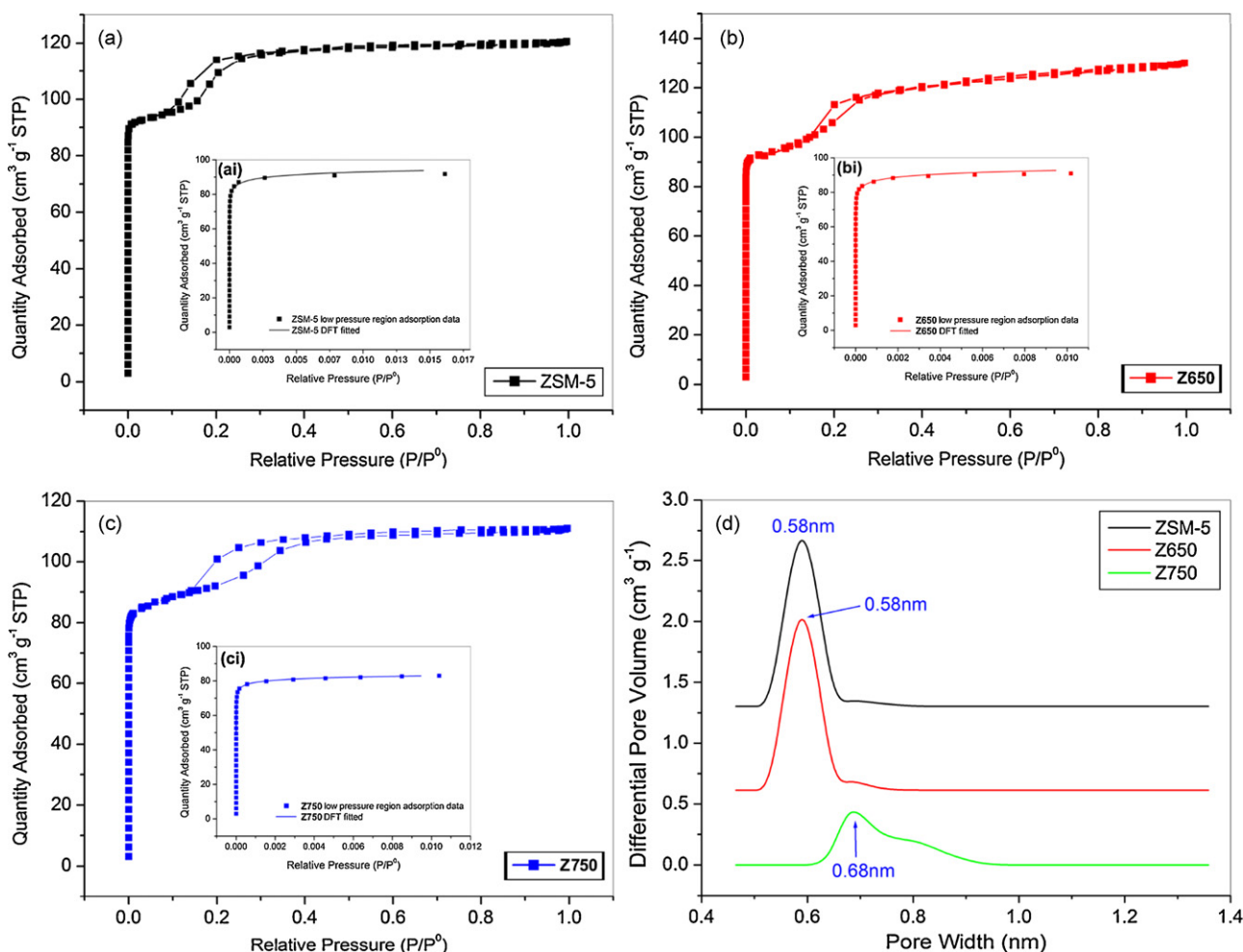


**Fig. 3.** Physisorption analysis of samples: (a–c)  $\text{N}_2$  adsorption isotherms at liquid  $\text{N}_2$  temperature; (ai, bi, ci) DFT model fitted curves in low pressure region; (d) microporous volume distribution analyzed by DFT method.

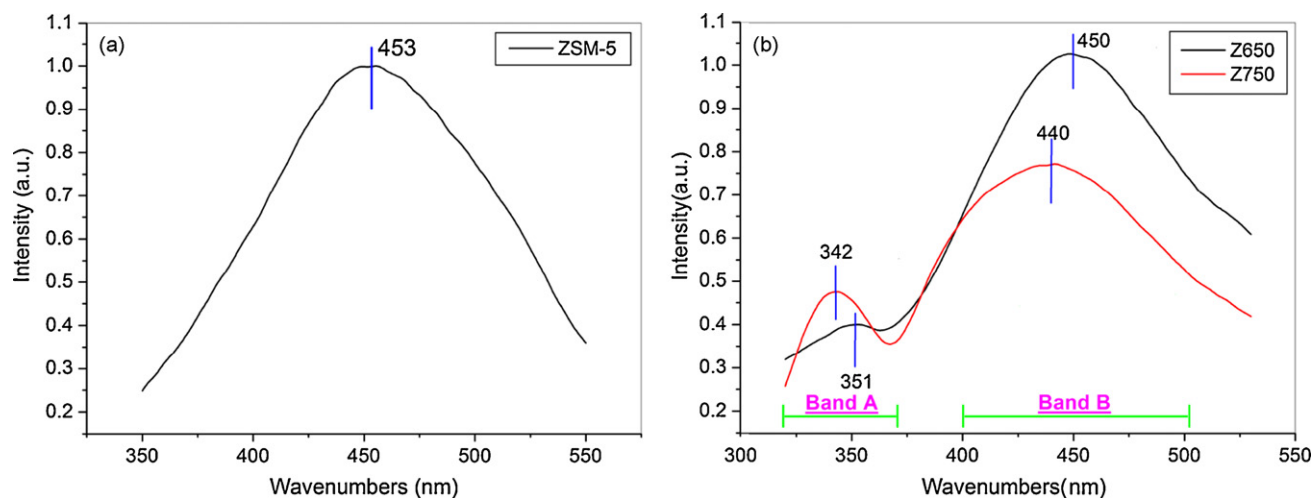


Fig. 4. Photoluminescence emission spectra (excited at 300 nm): (a) ZSM-5; (b) ZnO-loaded samples.

and then among the clusters some micropores with different sizes are newly produced. Thus, a broad distribution shoulder has been emerged.

Through DFT model, the micropore volume and surface area have also been obtained, listed in Table 1. Both micropore volume ( $V_{\text{micro}}$ ) and surface area in micropores ( $S_{\text{micro}}$ ) of Z650 sample is almost the same as ZSM-5 crystal. However, the two porosity parameters of Z750 sample present a reduction compared with the other two samples, particularly the  $S_{\text{micro}}$  value turns a sharp decrement. The results fully indicate that at 650 °C ZnO guests are mainly introduced into the external surface of ZSM-5 and the micropores are seldom occupied. While for Z750 sample, the micropores have been filled, resulting in the significantly decrease in the porosity value. The results obtained from  $V_{\text{micro}}$  and  $S_{\text{micro}}$  values are quite supportive to the conclusions received from isotherms and pore size distribution discussed above.

### 3.4. Photoluminescence

The normalized PL emission spectra (excited at 300 nm) of ZSM-5 crystals and ZnO-loaded samples are collected on PerkinElmer LS-55 instrument at room temperature, as shown in Fig. 4. The ZSM-5 crystals exhibit an emission band at 453 nm, which could not be determined till now because of the lack of evidence within literatures about PL emission properties of ZSM-5 crystals. Two emission bands, called Band A and Band B, are observed in the emission spectra of ZnO-loaded samples.

Band A at around 350 nm suggests that ZnO is formed in the channels of ZSM-5. Generally, the PL emission band of bulk ZnO appears around 370 nm. The blue shift here is attributed to small particle size effect yielded from the small particles encapsulated in the cages and channels of ZSM-5 frameworks. Meanwhile, it is demonstrated that the even smaller particles are formed in Z750 than in Z650, which is supported by the fact that the PL emission spectra of Z750 shifts to higher energy than Z650.

Whereas Band B, not a definite forming mechanism did researchers propose in previous reports. However, by making a comparison between the PL spectra of ZSM-5 crystals and ZnO-loaded materials, we could confirm that Band B is close related to the defects of host molecular sieves. Also, the infiltration of ZnO affects the emission center of the PL band to some extent, which turns a blue shift as the ZnO content increasing.

## 4. Conclusions

ZnO clusters have been successfully introduced into the pores of ZSM-5 crystals. A series of characterizations have been done to make sure that the clusters are surely encapsulated into the pores of ZSM-5. The intense porosity analysis is applied for the pore texture illustration. This material possesses good properties of visible light transmittance and photoluminescence, which could thereby be a good material for optical study and further use.

## Acknowledgements

The authors are grateful to Experimental Center of Chemistry, Dalian University of Technology (China) for providing the necessities in experiments. Many thanks are dedicated to Mr. Shouhua Ji and Mr. Longjiang Zou for their continuous support.

## References

- [1] J.H. Yang, J.H. Zheng, H.J. Zhai, L.L. Yang, Y.J. Zhang, J.H. Lang, M. Gao, J. Alloys Compd. 475 (2009) 741–744.
- [2] Y.X. Chen, B. Qu, Y.A. Barnakov, Q.L. Tang, J.H. Chen, J. Mater. Sci. Mater. El. 20 (2009) 328–333.
- [3] N. Combe, P.M. Chassaing, F. Demangeot, Phys. Rev. B 79 (2009) 045408.
- [4] J.H. Yang, X.Y. Liu, L.L. Yang, Y.X. Wang, Y.J. Zhang, J.H. Lang, M. Gao, M.B. Wei, J. Alloys Compd. 485 (2009) 743–746.
- [5] D.I. Son, Y.S. No, S.Y. Kim, D.H. Oh, W.T. Kim, T.W. Kim, J. Korean Phys. Soc. 55 (2009) 1973–1976.
- [6] C. Li, Z.S. Yu, S.M. Fang, H.X. Wang, Y.H. Gui, J.Q. Xu, R.F. Chen, J. Alloys Compd. 475 (2009) 718–722.
- [7] X.S. Zhu, J.X. Wang, X.Z. Zhang, Y. Chang, Y.S. Chen, Nanotechnology 20 (2009) 195103.
- [8] F. Wang, H.W. Song, G.H. Pan, L.B. Fan, Q.L. Dai, B.A. Dong, H.H. Liu, J.H. Yu, X. Wang, L. Li, Mater. Res. Bull. 44 (2009) 600–605.
- [9] A. Corma, H. Garcia, Chem. Commun. 13 (2004) 1443–1459.
- [10] W. Panpa, P. Sujaridworakun, S. Jinawath, Appl. Catal. B 80 (2008) 271–276.
- [11] C. Bouvy, B.L. Su, J. Mater. Sci. Technol. 24 (2008) 495–511.
- [12] C.S. Lim, J.H. Ryu, J. Cryst. Growth 311 (2009) 486–489.
- [13] C. Bouvy, E. Chelnokov, W. Marine, R. Sporken, B.L. Su, J. Non-Cryst. Solids 355 (2009) 1152–1156.
- [14] J. Wu, J. Zhu, Y. Shang, Y. Wang, R. Liu, C. Meng, Mater. Lett. 63 (2009) 1743–1746.
- [15] S. Brunauer, L.S. Deming, W.E. Deming, E. Teller, J. Am. Chem. Soc. 62 (1940) 1723–1732.
- [16] U. Muller, H. Reichert, E. Robens, K.K. Unger, Y. Grillet, F. Rouquerol, J. Rouquerol, D.F. Pan, A. Mersmann, Fresenius Z. Anal. Chem. 333 (1989) 433–436.